

UC Davis

UC Davis Previously Published Works

Title

The Surface Chemistry of Metal Oxide Clusters: From Metal–Organic Frameworks to Minerals

Permalink

<https://escholarship.org/uc/item/39m885zb>

Journal

ACS Central Science, 6(9)

ISSN

2374-7943

Authors

Yang, Dong
Babucci, Melike
Casey, William H
[et al.](#)

Publication Date

2020-09-23

DOI

10.1021/acscentsci.0c00803

Peer reviewed

The Surface Chemistry of Metal Oxide Clusters: From Metal–Organic Frameworks to Minerals

Dong Yang, Melike Babucci, William H. Casey, and Bruce C. Gates*



Cite This: *ACS Cent. Sci.* 2020, 6, 1523–1533



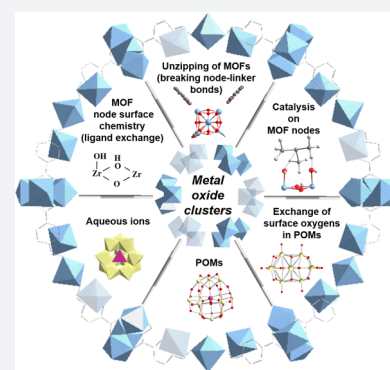
Read Online

ACCESS |

Metrics & More

Article Recommendations

ABSTRACT: Many metal–organic frameworks (MOFs) incorporate nodes that are small metal oxide clusters. Some of these MOFs are stable at high temperatures, offering good prospects as catalysts—prospects that focus attention on their defect sites and reactivities—all part of a broader subject: the surface chemistry of metal oxide clusters, illustrated here for MOF nodes and for polyoxocations and polyoxoanions. Ligands on MOF defect sites form during synthesis and are central to the understanding and control of MOF reactivity. Reactions of alcohols are illustrative probes of Zr_6O_8 node defects in UiO-66, characterized by the interconversions of formate, methoxy, hydroxy, and linker carboxylate ligands and by catalysis of alcohol dehydration reactions. We posit that new reactivities of MOF nodes will emerge from incorporation of a wide range of groups on their surfaces and from targeted substitutions of metals within them.



1. METAL OXIDE CLUSTERS IN METAL–ORGANIC FRAMEWORKS

Metal–organic frameworks (MOFs) are regular open matrices consisting of inorganic nodes linked by organic struts.^{1–3} With their often stunning structures, these materials command wide attention in the chemical community today. MOF discovery has been thought of as a search to expand the coordination structures of metal complexes into space by adding repeat units to the structures.⁴ Building from the early examples of 3D MOFs with permanent porosity reported in 1999—HKUST-1—by Williams’ group⁵ and the high-surface-area MOF-5—by Yaghi’s group (Figure 1)—researchers have now created more than 80 000 MOFs,⁷ with new ones reported almost daily and colossal opportunities for discovery of still more, with chemical functionalities positioned precisely in structures having thousands of square meters per gram of internal surface area.³

Early reports of MOFs were dominated by images of fascinating reticular structures (e.g., MIL-53, MIL-101, MIL-125, and UiO-66; Figure 1). As MOF science matured beyond the search for new structures, researchers increasingly sought MOFs with exploitable properties, such as for selective gas separations and for catalysis. Catalysis is especially challenging because it requires materials with functionality optimized for transport, chemisorption, reaction, and desorption, whereas separations require only optimized transport and adsorption/desorption. Catalytic sites can be built onto MOF nodes and linkers for controlled spacing of complementary groups.

In the search for useful catalysts, researchers have been drawn to MOFs that are stable for use at high temperatures—in the MOF, MIL, and UiO families. These have nodes that are

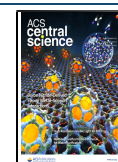
metal oxide clusters, such as $M(OH)$ chains ($M = Al, Cr, Fe, Ga, In$), M_4O ($M = Zn$), M_3O ($M = Al, Fe, Cr$), $M_6O_4(OH)_4$ ($M = Zr, Hf, Ce$), $M_8O_8(OH)_4$ ($M = Ti$) (Figure 1), and $M_4(OH)_4$ ($M = Ni, Co$).^{6,8–11} These clusters are essentially molecular, and so they tempt researchers to find links to nature’s catalysts that incorporate molecular clusters, exemplified by Mn_4CaO_5 in photosystem II for water splitting to release O_2 .¹² Heterogeneous catalysis scientists naturally compare metal oxide clusters in MOFs with bulk metal oxides, which find wide industrial application as catalysts and catalyst supports.

2. SURFACE CHEMISTRY OF MOF METAL OXIDE CLUSTER NODES

In some defect-free MOF structures, open sites are identified as isolated regular structural vacancies, illustrated by those on the M_3O nodes of MIL-101 (Figure 1). Other node sites not occupied by linkers are defects (illustrated for UiO-66 in Figure 2). In any MOF, there are imperfections—defects—where linkers (and/or nodes) are missing. Defects and the related crystal disorder are a significant branch of MOF science.^{13,14} The ideal (defect-free) structures of NU-1000 and of MOF-808, for example, have 4 and 6 of the 12 sites on each

Received: June 18, 2020

Published: August 6, 2020



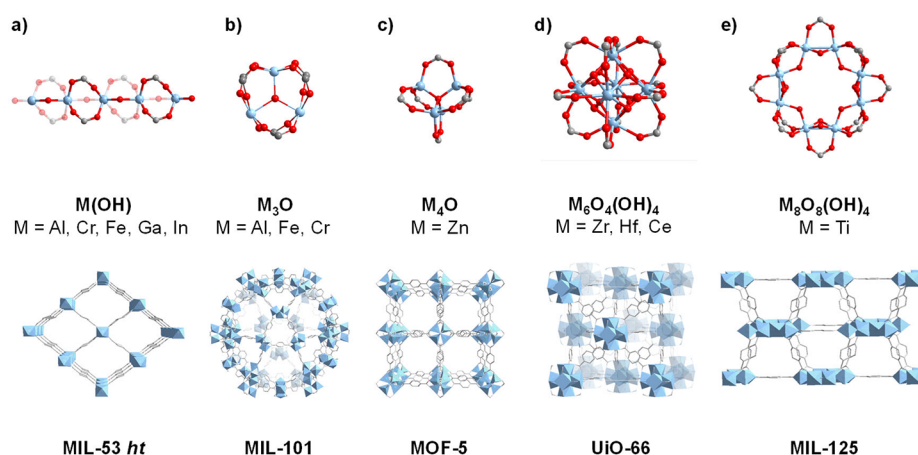


Figure 1. Illustrations of metal oxide node structures and crystal structures of five MOFs that incorporate benzene-1,4-dicarboxylate (BDC^{2-}) linkers: (a) MIL-53 *ht*, (b) MIL-101, (c) MOF-5, (d) UiO-66, and (e) MIL-125. Color code: metal atoms and metal–oxygen polyhedra (light blue), oxygen (red), carbon (gray).

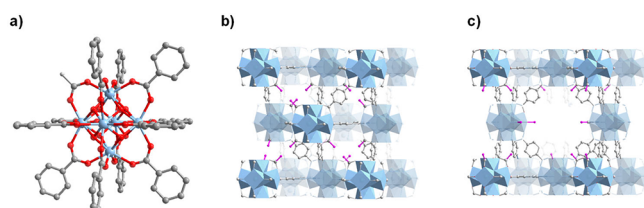


Figure 2. (a) Structure of UiO-66 emphasizing, at left, locations of individual atoms and missing linker defects where formate ligands are bonded, each to two Zr sites (BDC^{2-} linkers are truncated for simplicity). (b) Illustration of missing linker defects of UiO-66. (c) Illustration of missing node defects of UiO-66. Color code: Zr atoms and ZrO_8 octahedra (light blue), oxygen (red), carbon (gray), hydrogen (white), formate ligands (purple) in parts b and c. Adapted and reprinted with permission from ref 19. Copyright 2016 American Chemical Society.

Zr_6O_8 node, respectively, open, not occupied by linkers, and these structural vacancies have identities/ligands similar to those of defect sites. The defect sites in our examples are paired sites where bidentate carboxylate linkers typically bond. In reactions involving gas-phase reactants and MOF nodes, the distinctions in reactivity between node structural vacancies and defects are not clear. In contrast to the MOF nodes in the presence of gas-phase reactants, metal oxide clusters in water are generally coordinatively saturated (more about this below).

Our main focus is on the reactivities of node defect sites, and we see this as part of a broader subject: the *surface chemistry of metal oxide clusters*, illustrated here for MOF nodes and also for polyoxometalates (POMs), which have long been designed to have targeted defects. We posit that an understanding of POM chemistry may help elucidate MOF chemistry.

MOFs in the family we emphasize are synthesized as (1) metal oxide clusters form from metal salts in solution and then (2) self-assemble into matrices by combining with linkers that have carboxylate groups at multiple ends. Each carboxylate group can bond with a pair of neighboring metal sites on a node. Various linker structures combine with the nodes to give various reticular structures (Figure 1).

In some representations (e.g., Figure 1), the structural vacancies are shown as open sites, but during synthesis they usually become occupied by ligands from the synthesis

solution, typically remaining in place in the final crystalline structure (Figure 2).

What are these native nonlinker ligands? Debates about them are ongoing, because they are not always easy to identify—they may be few in number and irregularly placed, so that information about them does not emerge from X-ray diffraction (XRD) crystallography. Many researchers have suggested that these ligands include hydroxy and aqua from the aqueous synthesis mixtures; specific suggestions include hydrogen-bonded pairs of OH/OH₂ groups;^{15,16} OH/OH₂/OH₂;¹⁷ and carboxylates other than linkers.^{18,19}

The identities of these original ligands on the nodes depend on the compositions of the synthesis solutions, which often include modulators—components added to facilitate the slow, regular formation of high-quality MOF crystals. The modulators also influence the number of defect sites per node. Typical modulators in UiO-66 synthesis are monocarboxylic acids (e.g., formic acid, acetic acid) and HCl.^{20,21} The former leave carboxylate ligands on the nodes;¹⁹ formate ligands also form from decomposition of dimethylformamide (DMF) used in the synthesis solutions,¹⁹ and these account for the majority of nonlinker ligands on the nodes when HCl is used as a modulator.²²

Understanding the chemistry of these ligands and the node sites where they bond is central to understanding MOF catalysis. The original ligands can be replaced by others, and in catalysis, there will be a dynamic competition for the node surface sites where catalysis occurs. An understanding of node surface chemistry is emerging for some MOFs (Figure 3). There is broad flexibility in the chemistry of ligand replacement on the nodes, with either liquid-phase or vapor-phase reactants. For example, solvent-assisted ligand incorporation leads to switching of carboxylate or phosphonate ligands on Zr_6O_8 nodes of UiO-66 and NU-1000.^{23,24} Reaction with methanol converts carboxylate ligands on the node defects via esterification, with ester desorbed as a product and OH ligands remaining on the nodes and reacting further with methanol to form (monodentate) methoxy ligands (Scheme 1).^{22,25,26} The methoxy groups can be reversibly replaced by terminal OH groups by reaction with water vapor, with methanol desorbed as a product (Scheme 1). Methoxy and hydroxy ligands tend to be more reactive than carboxylate ligands, and so reactant molecules can displace them to initiate catalysis (Scheme 1).

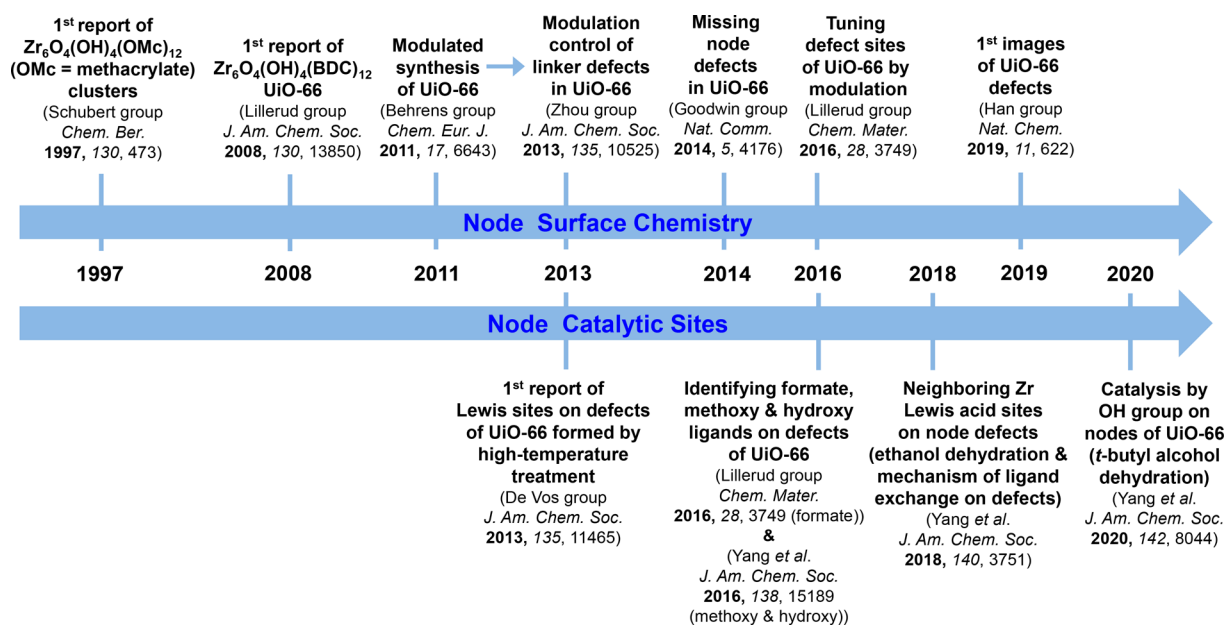
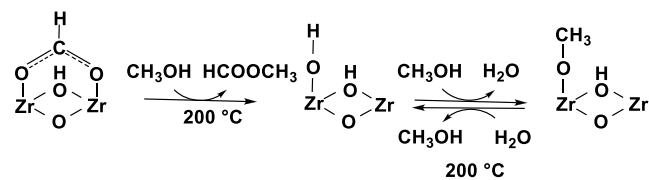


Figure 3. Timeline of advances in the understanding of open sites, defects, ligands, and reactivities on MOF node surfaces illustrated for UiO-66. The key role of MOF defects for catalysis was proposed in 2008, as Farasseng's group investigated alkylation of biphenyl with *t*-butyl chloride catalyzed by MOF-5;²⁷ this work appeared nine years after the first synthesis of that MOF.⁶ The group synthesized MOFs by fast precipitation and used dummy linkers to create node defect sites, confirming that these are catalytic sites for toluene benzylation.²⁸ In 2016, they summarized progress in understanding MOF defects as catalytic sites.²⁹ UiO-66 has Zr_6O_8 nodes, each bonded in the defect-free MOF to 12 BDC²⁻ linkers, as reported by Lillerud's group.⁸ That work underlies the emergence of a family of MOFs made with various linkers.³⁰ The highly tunable defect structures are central to catalysis by these MOFs. In 2011, benzoic acid and acetic acid were first used as modulators in UiO-66 synthesis.²⁰ Two years later, Zhou's group³¹ found that the synthesis modulated by acetic acid provided opportunities to tune missing linker defects, with the number correlated with MOF BET surface areas. In 2014, the group of Goodwin³² found high concentrations of missing node defects with *reo* topologies in Hf-UiO-66 synthesized with formic acid modulator, made evident by XRD patterns. Then, two types of defects had been identified, missing linker and missing node defects. Lillerud's group in 2016 reported¹⁹ the tuning of defects in UiO-66 by addition of modulators with different pKa values, and they quantified the number of defects by applying thermal gravimetric analysis, ¹H NMR spectroscopy of dissolved MOFs, BET surface area measurements, and XRD crystallography. At an early stage, it was concluded that MOF defect sites are the Lewis acid catalytic sites for several acid-catalyzed reactions, for example, in MOF-5²⁸ and in UiO-66.¹⁸ Activating the nodes as catalysts may be as simple as removal of the ligands.¹⁸ Lillerud's group¹⁹ in 2016 showed by IR spectroscopy of MOFs and ¹H NMR spectroscopy of digested MOFs that the original ligands include both carboxylates from modulators and formate from decomposed DMF solvent.^{22,25,33} Alcohols were used as probe molecules to investigate the catalytic properties of sites on Cr_3O nodes of MIL-100,³⁴ and methanol was used to probe sites in UiO-66.²⁶

Scheme 1. Schematic Representation of Node Chemistry during Reaction of As-Synthesized UiO-66 (Formate) with Methanol Demonstrating Conversion of Carboxylate Ligands into Terminal OH Groups via Esterification (Further Reaction with Methanol Forms Monodentate Methoxy Ligands)



Esterification reactions are crucial for these ligand exchanges, and experiments have shown that carboxylate ligands are quite stable in the presence of water vapor.

The understanding of node surface chemistry paves the way to the understanding of mechanisms of catalytic reactions on the nodes, and density functional theory (DFT) is essential for elucidating details and predicting reactivities.³⁵ For example, ethoxy ligands, formed from vapor-phase ethanol and observed spectroscopically, were found by DFT to be bonded to Lewis acid defect sites on UiO-66 and to be intermediates in the catalytic dehydration to make diethyl ether. A key step is the

breaking of node–linker bonds (or the accidental adjacency of open node sites) allowing catalytically fruitful bonding of two reactant species to neighboring node sites, facilitating an S_N2 mechanism.²² The Zr Lewis acid sites also catalyze hydrolysis of nerve gas simulants,³⁶ among other reactions.^{37,38}

A complementary catalytic probe reaction is the dehydration of *t*-butyl alcohol (TBA) present in the vapor phase, which gives isobutylene, but no ether. This reaction is catalyzed by OH groups on Zr_6O_8 nodes in UiO-66 and in MOF-808. Experiments and DFT calculations show that (1) terminal node OH groups form as formate and/or acetate ligands present initially on the nodes react with TBA to form esters; (2) these OH groups act as Brønsted base sites for TBA dehydration, facilitating the reaction via a carbocationic intermediate in an E1 mechanism (Figure 4).²⁵

The understanding of the node chemistry of MOFs such as UiO-66 is pointing the way to predicting the reactivities of MOFs that have nodes with various structures. For example, *hcp* UiO-66 incorporates double layered Zr_6O_8 nodes bridged by $6 \mu_2$ -OH groups ($Zr_{12}O_{22}$).³⁹ These nodes lend themselves to tuning: when *hcp* UiO-66 is synthesized with nodes incorporating acetate ligands where linkers are missing, catalysis is inhibited, but when the acetate is removed by reaction with methanol to split out methyl acetate and form methoxy ligands on the nodes, catalysis of epoxide ring

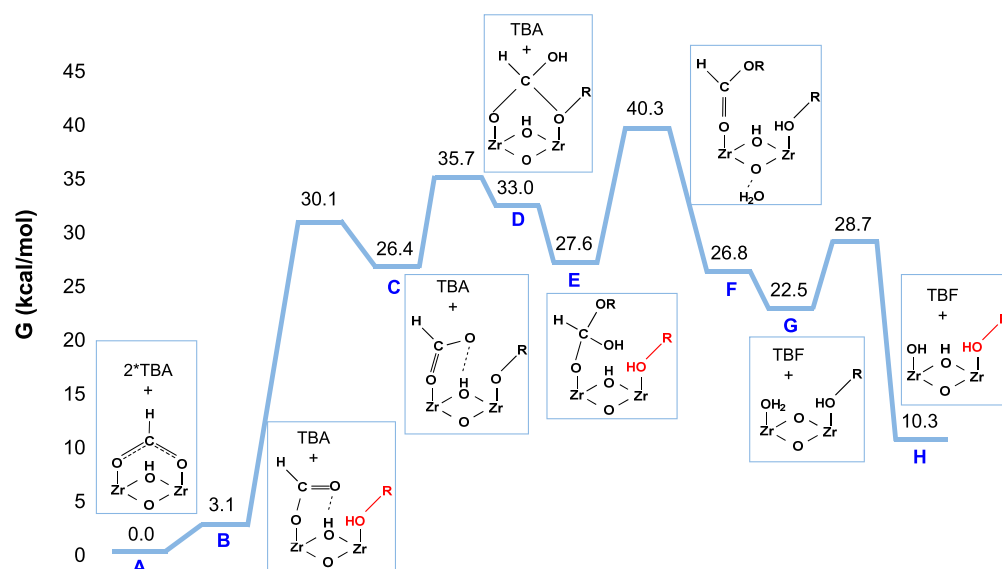
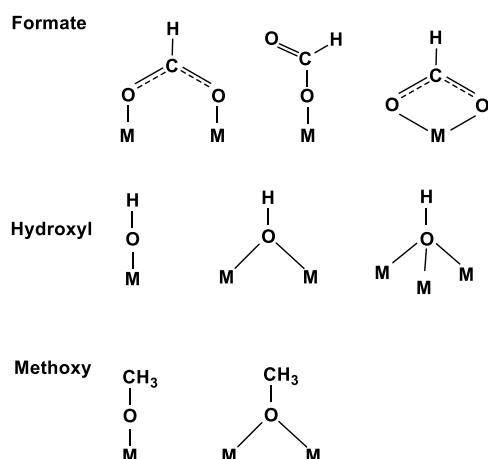


Figure 4. Free energy reaction profile for the esterification reaction between formate and *t*-butyl alcohol (TBA) on UiO-66 nodes, followed by catalysis of TBA dehydration.²⁵ (A) UiO-66 having formate bonded to zirconium sites. (B) One zirconium bonding site opened for binding with one TBA molecule. (C) TBA interacting with a zirconium site. (D) OR group (R: *t*-butyl) acting as a nucleophile and attacking the C atom of the formate. (E) Second TBA molecule binding to the zirconium site. (F) OH group removed, forming water and *t*-butyl formate (TBF). (G) TBF removed, water bonding to the zirconium site. (H) TBA and a terminal OH group (formed after esterification) bonding to zirconium atoms. The alcohol molecules bonded to zirconium and the OH group formed after esterification are highlighted in red.²⁵ Adapted with permission from ref 25. Copyright 2020 American Chemical Society.

opening with alcohols starts up. The defects on $Zr_{12}O_{22}$ nodes are several times more active per site than those on Zr_6O_8 nodes, a result that suggests that the bridging OH groups increase the catalytic activity of the neighboring sites.

The hydroxy, formate, and methoxy species that are important in this MOF node chemistry also exist on bulk metal oxides (Scheme 2), and they are important for

Scheme 2. Formate, Methoxy, and Hydroxy Groups Identified Spectroscopically on Surfaces of Bulk Metal Oxides



understanding the surface chemistry of those materials⁴⁰—however, they are usually present in mixtures,^{41–43} in contrast to the individual species made in high purity on MOF node defect sites.^{22,25}

The structures of the species bonded to the nodes are dictated by the essentially molecular structures of the nodes—

influenced, for example, by the sizes of the node metal atoms and the distances between them. The uniformity of MOF metal oxide nodes facilitates the precise determination of how the ligands are bonded, forming a strong foundation for understanding how catalysis occurs. Examples of catalysis on MOF nodes may emerge as some of the best understood of any in heterogeneous catalysis.

We foresee rich opportunities to extend the chemistry of MOFs having metal oxide cluster nodes, and there are already numerous examples. Thus, the nodes have been used as platforms for various catalytic groups, such as sulfates with nearby aqua ligands that function as strong Brønsted acids.⁴⁴ Transition metal complexes have been anchored to the nodes;^{45,46} rhodium *gem*-dicarbonyls and iridium *gem*-dicarbonyls are subtle probes of the node surfaces, their ν_{CO} infrared spectra demonstrating that the node surface sites are less uniform than was first expected^{47–50} and thus providing early hints of subtlety of node surface chemistry.

The node surface chemistry can be tuned by varying the compositions of the linkers. For example, NH_2 groups added to the BDC linkers of UiO-66 increase the catalytic activity of the MOF for the hydrolysis of warfare agent simulants.^{51,52}

MOF nodes comprising mixtures of metals also offer intriguing prospects. We may view these as nodes with defects. Research with MOFs having mixed-metal nodes is potentially important for catalysis because it suggests ways to tune the properties of the nodes to mimic nature (consider the Mn_4CaO_5 clusters in photosystem II or the effect of heterometals in POMs, mentioned below).^{53,54} Various methods (e.g., modified syntheses or postsynthesis ion exchange) have been reported for the synthesis of MOFs with combinations of metals in the nodes,^{55–59} exemplified by dimeric iron in the linear $Al(OH)$ node of MIL-53 for the challenging methane to methanol conversion.⁶⁰ However, MOFs with mixed metal nodes are not simple to make, with

syntheses often leading to mixtures of amorphous metal oxides along with MOFs.^{61–63} Successful syntheses require an optimal balance between hydrolysis chemistry influencing cluster formation and coordination chemistry involving nodes and ligands that provide sufficient rigidity.

3. STEPS TOWARD MIMICKING ENZYME METAL OXIDE CLUSTER CHEMISTRY IN MOFS

Attempts to find links between metal oxide clusters in enzymes and those in MOFs are at an early stage. The aforementioned Mn_4CaO_5 has triggered work on cubane complexes with the core structure of M_4O_4 ($\text{M} = \text{Co}, \text{Ni}, \text{Co/Ni}, \text{or Co/Mn}$).^{64–67} These have been incorporated into MOFs as nodes and have been shown to have activity for oxygen evolution.^{11,68} The mechanism is not yet understood, but it has been suggested that hydroxy groups play a role in the catalytic process, being converted reversibly to oxo sites via two-electron reactions.^{69–71}

This is lively research that is rich in opportunity. The natural oxide structure of divalent metals undergoing hydrolysis is that of the brucite layer structure made of linked cubane moieties. Linked cubane structures also form from tetravalent metals such as Mn(IV) , and, then, they resemble defective birnessite (MnO_2). Sandwich polyoxometalates and cubane synthesis strategies produce these layered fragments, and dynamics of the layer may be essential to catalytic cycles.⁷⁰

4. SURFACE CHEMISTRY OF AQUEOUS METAL OXIDE CLUSTERS

Some MOFs with metal oxide cluster nodes are formed directly in aqueous solution. For example, the long-rod Al(OH) nodes of MIL-53,⁷³ among others, are formed in DMF, but only in the presence of water; another example is the Zr_6O_8 nodes of UiO-66.²⁰ However, water can also damage MOF structures—some MOFs (e.g., MIL-125) with metal oxide nodes are unstable in aqueous media.⁷⁴ Here, the extensive work on water-oxidation catalysis by mineral-like cubanes is relevant,⁶⁸ showing that the choice of ligands is essential for catalyst stability, whether they are organic, as for cubanes, or inorganic, as for POMs.^{68,75,76} A challenge in this work is to ligate metals so that the cluster maintains integrity during repeated redox cycles.^{68,69,72}

Investigations of oxo-site reactivities in unbound Zr(IV) clusters, such as $[\text{Zr}_4(\text{OH})_8(\text{OH}_2)_{16}]^{8+}$ tetramers in aqueous solution,⁷⁷ have provided evidence of sites similar to those on Zr_6O_8 MOF nodes.⁴⁴ The comparisons are imperfect because the unbound clusters are not structurally the same as these nodes, but the comparisons are good enough to be useful for understanding ligand exchanges and assigning Brønsted acidities.

Better models of metal oxide clusters are molecules for which the structures in aqueous solution are known with confidence. Extensive work has been done on the polyoxoanions of Group 5 and Group 6 oxides and the polyoxocations incorporating trivalent metals (e.g., Al(III) , Fe(III) , Ga(III)). The clusters are typically ~ 1 nm in diameter and incorporate a few dozen to a few hundred atoms. The POMs as a class, usually of Group 6 metals, are acid-, oxidative-, photo-, and electrocatalysts⁷⁸ and are targets for photoenergy production.^{79,80} Wide ranges of defect (e.g., lacunary) and sandwich structures of these have been synthesized, and their catalytic chemistry is well reviewed.⁸¹

The cationic clusters of Group 13 metals provide a link to the aqueous surface chemistry of common soil minerals, such as the layered minerals mentioned above, because they are often structurally related (Figure 5). The oxide minerals in

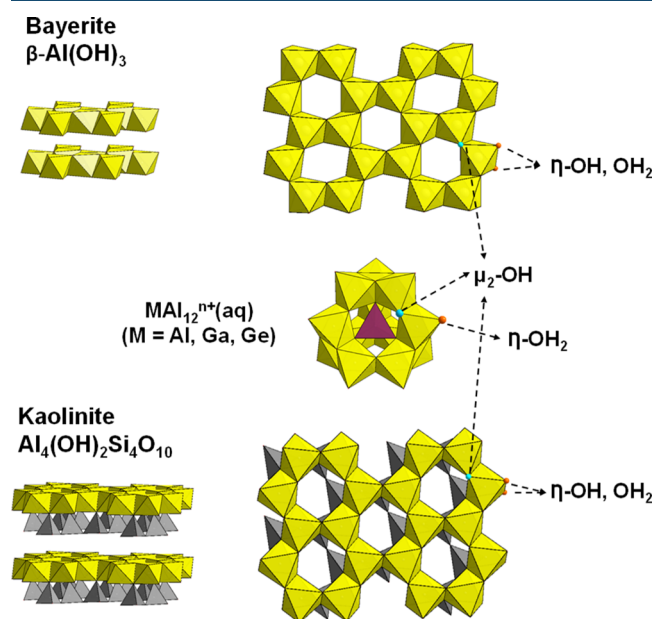


Figure 5. Aluminum polyoxocation structures shown in polyhedral representation along with a common aluminum hydroxide mineral and the clay mineral kaolinite. The aqueous Keggin $[\text{MO}_4\text{Al}_{12}(\text{OH})_{24}(\text{OH}_2)_{12}]^{7/8+}$ ion is in the center, with the purple tetrahedron indicating the inert M(O)_4 site. Gray tetrahedra are $[\text{SiO}_4]^{4-}$; yellow octahedra are $[\text{Al(O)}_6]^{9-}$.

water are often layer minerals that are characterized by pH-dependent surface charges, by the formation of coordination complexes with ligands and with other metals, and by catalytic properties attributed to defect sites.

To address subtle effects in the chemistry, researchers have modified the clusters by single-metal-atom substitutions (and, separately, some ligand substitutions) and determined how they affect reactions on the surfaces.⁸² Examples are cationic clusters of the ϵ -Keggin class, including $[\text{MO}_4\text{Al}_{12}(\text{OH})_{24}(\text{OH}_2)_{12}]^{7/8+}$ (abbreviated MA_{12} with $\text{M} = \text{Al(III)}, \text{Ga(III)}, \text{Ge(IV)}$),^{78,81} because they are similar to some aluminum-(hydr)oxide minerals and because details of their surface chemistry link them to MOF nodes.⁸³ The use of metal substitutions to modify structures and acid–base and electronic properties of POMs is a well-developed field.⁸⁴ In some cases, second-shell interactions are essential to stabilize the POMs (e.g., certain isomers) either via co-ion coordination to the cluster or by ligation.^{85–89}

The clusters incorporating trivalent metals are amphoteric in water and have a rich Brønsted acid–base chemistry, in contrast to the Group 5 and 6 Keggin anion clusters, which are the conjugate bases of stronger acids. The Group 13 Keggin polyoxocations have surface μ_2 -OH groups and reactivities for isotope exchange that are highly sensitive to small changes in structure and composition. These exchanges proceed by transient formation of metastable open structures,⁸² these cations are comparable to the defective MOF nodes. Metals are usually coordinatively saturated in a mobile solvent like water. Structural oxygens in the lattice, however, exhibit a range of coordination numbers. The oxygen coordination

numbers typically become smaller as a stable cluster partly opens to form a defect.

In contrast to the μ_2 -OH groups, terminal aqua ligands (η -OH₂) in MAI₁₂ undergo ligand exchange at rates that are only slightly insensitive to small changes in the cluster structure.^{90–92} The rates also change with charge on the cation cluster, and rates of reactions, particular at bridges, can be modified by fluoride-for-oxygen substitution⁹³ in the lattice or at terminal sites. Investigations of Group 5 polyoxoanions largely confirm the view that equilibria with partly open defective forms of the stable condensed clusters control the rates of oxygen-isotope exchanges.^{94,95} The rates of steady oxygen-isotope exchange of the structural oxo sites, which include two sets of $\eta=O$, three sets of μ_2-O , one set of μ_3-O , and one inert set of μ_6-O , vary by $>10^4$ -fold. Ti(IV) for Nb(V) substitution changed the pH dependencies of the molecule, leading to broad amphoteric behavior, but all oxygen sites exhibited a broadly similar pH dependence as though the formation of a partly detached defect structure controlled the rates for all oxygens.

Comparing the surface chemistries of these polyoxoanions and polyoxocations with those of the MOF nodes, we see similarities in the reactions of hydroxy and aqua ligands, but the comparisons are lacking in detail, in large part because some of the most insightful POM data involve reactions in aqueous media. Such chemistry is not the most relevant to the reactions of MOFs with vapor-phase reactants and when open coordination sites can be maintained on the metals. However, recent work is providing some closer links; for example, by reacting trivacant lacunary Keggin-type POMs in organic solvents with methanol, six methoxy groups were introduced into the vacant sites of each.⁹⁶

5. METAL OXIDE CLUSTERS WITHIN LARGER CLUSTERS, DISPERSED ON SUPPORTS, AND LINKED IN FRAMEWORKS

One might also ask whether data characterizing POMs isolated in dispersed form in solid phases might provide better comparisons with MOF nodes than those stated above. The literature of clusters of POMs (clusters of clusters) illustrates a wide variety of open structures made from POM building blocks—and some comparisons with MOFs.⁸³ There is also a substantial literature of POMs on supports,⁹⁷ of interest to the heterogeneous catalysis community⁹⁸ because they are catalysts for acid–base^{99–101} and redox reactions.^{78,102,103} The reactivities are essentially as one would expect on the basis of what we have summarized here, but the data lack the detail to provide close links to MOF node chemistry.⁸³ Part of the challenge in elucidating the chemistry of supported POMs lies in the complexity of their structures—they are typically aggregated and structurally ill-defined.^{83,104,105}

Better comparisons might be with MOFs that contain POMs as nodes; these are called POM–organic frameworks (POMOFs).^{83,106,107} Well-established examples incorporate ϵ -Keggin POM $\{\epsilon\text{-P}M_o^V_8M_o^VI_4O_{40-x}(OH)_xM_4\}$ (abbreviated as ϵ -M₄PMo₁₂, M = Zn or La), in which the four M atoms at corners of POM clusters are connected with BDC or benzene-1,3,5-tricarboxylic acid (BTC) linkers.^{108,109} However, these samples are not stable; the La-containing POMOF gradually collapses at room temperature, and the Zn-containing POMOF survives only at temperatures up to 180 °C.^{108–110} Some POMOFs are more stable; for example, that with a $[\text{Ni}_6(\mu_3\text{-OH})_3(\text{H}_2\text{O})_6(\text{L})_3(\text{B-}\alpha\text{-PW}_9\text{O}_{34})]$ node (abbreviated

as Ni₆PW₉, L = en/enMe) and BTC linkers can survive at temperatures up to 320 °C.¹¹¹ However, these POMOFs are still much less stable than the most stable MOFs. For example, UiO-66(Zr) and MIL-53(Al) are stable at 400 and 500 °C, respectively,^{73,112} because (1) only few metal atoms (not all of them) in POMs are coordinated with linkers, (2) the metal–linker bonds in POMOFs are less strong than those in these MOFs, and (3) anionic POM nodes need large organic cations to balance the charges, and these take up space in the pores and weaken the linkage bonds.

Only a few POMs have been successfully applied as POMOF nodes. Progress is limited by discovery and understanding of the chemistry of bonding of POMs with organic ligands and how to control the chemistry of linking POMs into POMOFs in solution.

As on POMs, oxo and hydroxy groups are common on the nodes of POMOFs; however, their reactivities are almost unexplored. This field is still in an early stage and developing rapidly, and we foresee opportunities for applying these materials as catalysts.

6. COMMON THREADS OF METAL OXIDE CLUSTER SURFACE CHEMISTRY

To summarize a few points, MOFs are linked metal complexes that have many catalytic properties in common with molecular catalysts in solution, and node surfaces are often crucial. The metal oxide clusters in solution that most resemble MOF node clusters are POMs, and investigations of these emphasize that transient defect structures are often important.

A common characteristic links metal oxide clusters in MOFs and POMs in solution: both are protected to limit cluster aggregation—the former by linkers and the latter by ionization and polar, aqueous surroundings. Both kinds of clusters tend to aggregate when these protective surroundings are removed.

A common characteristic links metal oxide clusters in MOFs and POMs in solution: both are protected to limit cluster aggregation—the former by linkers and the latter by ionization and polar, aqueous surroundings.

Rates of ligand exchanges in POMs are sensitive to both the metal in the clusters and the ligands, and the same is true for MOF nodes.¹¹³ Thus, MOFs incorporating high-valent metal ions form strong coordination bonds with linkers for good MOF stability,¹¹⁴ and MOFs having nodes that incorporate metals with variable oxidation states, like POMs, are active for catalytic redox reactions,¹¹⁵ offering rich opportunities for discovery.^{104,116} Heterometal or anion substitution into Keggin ions profoundly affects stabilities and reactivities, particularly when those substitutions are into sites that strongly influence the metastable equilibria with defective forms. The addition of a more highly charged heterometal atom to a Keggin ion (e.g., P(V) for Si(IV) in tungstate Keggin ions) can stabilize different isomers and lacunary forms and make stronger acids.^{84,117,118} Extension of these effects to MOF nodes, however, has limitations: the MOF nodes with high-valent metal ions are typically much less stable than comparable

nodes incorporating metals in nonvariable oxidation states that undergo reductive dissociation.¹¹⁹

Rates of ligand exchanges in POMs are sensitive to both the metal in the clusters and the ligands, and the same is true for MOF nodes.

Like bulk metal oxides, metal oxide clusters in MOFs and POMs are able to bond with numerous ligands, exemplified by methoxy and hydroxy. These ligands on metal oxide clusters may play charge-balancing roles—or just fill the vacancies; they may be bonded in various forms (Figure 5), and dynamic simulations indicate that ligand substitutions sometimes do not have a simple effect on reactivity.⁹⁵ Much remains to be learned about the chemistry of ligands and the surfaces of metal oxide clusters.

7. OUTLOOK/PERSPECTIVE

As MOF chemistry expands, there are emerging opportunities to understand and control reactivities of MOFs having metal oxide cluster nodes and to take advantage of known chemistry of metal oxide clusters such as POMs. Ligands, such as formate, methoxy, and hydroxy, are common to bulk metal oxides, metal oxide clusters in MOFs, and POMs, and understanding of the chemistry of these and other ligands on the surfaces of these materials may be expected to play a central role in unraveling the adsorption and catalytic properties of all of them. There is much to learn about what determines the bonding of ligands to metal oxide clusters and how it influences reactivities. Thus, we suggest that there are rich opportunities to better understand the chemistry of MOFs and to design metal oxide cluster nodes for reactivity, catalysis, and even selective adsorption using DFT and some of the tools derived from POM chemistry. And, although this is highly challenging, there is also a wide horizon for discovery of new MOFs with nodes including clusters of oxides with various metals, and other clusters such as sulfides as nodes.

Understanding of the surface chemistry of ligands, such as carboxylate, alkoxy, and hydroxy, on metal oxide clusters in MOFs and POMs plays a central role in unraveling the adsorption and catalytic properties of these materials.

AUTHOR INFORMATION

Corresponding Author

Bruce C. Gates – Department of Chemical Engineering, University of California, Davis, California 95616, United States; orcid.org/0000-0003-0274-4882; Email: bcgates@ucdavis.edu

Authors

Dong Yang – Department of Chemical Engineering, University of California, Davis, California 95616, United States; College of Chemical Engineering, Nanjing Tech University, Nanjing, Jiangsu 21000, China

Melike Babucci – Department of Chemical Engineering, University of California, Davis, California 95616, United States; orcid.org/0000-0001-7785-3755

William H. Casey – Department of Earth and Planetary Sciences and Department of Chemistry, University of California, Davis, California 95616, United States; orcid.org/0000-0002-3275-6465

Complete contact information is available at:
<https://pubs.acs.org/10.1021/acscentsci.0c00803>

Author Contributions

The manuscript was written through contributions of all authors. All authors have given approval to the final version of the manuscript.

Notes

The authors declare no competing financial interest.

ACKNOWLEDGMENTS

This work was supported as part of the Inorganometallic Catalyst Design Center, an Energy Frontier Research Center funded by the U.S. Department of Energy (DOE), Office of Science, Basic Energy Sciences (BES), Chemical Sciences, Geosciences, and Biosciences Division (DE-SC0012702) (M.B., B.C.G.) and by a DOE BES Chemical Sciences, Geosciences, and Biosciences Division grant (DE-FG0205ER15693) (W.H.C.). D.Y. thanks the “Distinguished Professor” program (2018) and the “Innovative and Entrepreneurial Talent” program (2019) of Jiangsu province and the Priority Academic Program Development of Jiangsu Higher Education Institutions (PAPD) for funding.

REFERENCES

- (1) Férey, G. Hybrid porous solids: past, present, future. *Chem. Soc. Rev.* **2008**, *37*, 191–214.
- (2) Horike, S.; Shimomura, S.; Kitagawa, S. Soft porous crystals. *Nat. Chem.* **2009**, *1*, 695–704.
- (3) Furukawa, H.; Cordova, K. E.; O’Keeffe, M.; Yaghi, O. M. The Chemistry and Applications of Metal–Organic Frameworks. *Science* **2013**, *341*, 1230444–1230455.
- (4) Diercks, C. S.; Kalmuzki, M. J.; Diercks, N. J.; Yaghi, O. M. Conceptual Advances from Werner Complexes to Metal–Organic Frameworks. *ACS Cent. Sci.* **2018**, *4*, 1457–1464.
- (5) Chui, S. S.-Y.; Lo, S. M.-F.; Charmant, J. P. H.; Orpen, A. G.; Williams, I. D. A Chemically Functionalizable Nanoporous Material [Cu₃(TMA)₂(H₂O)₃]_n. *Science* **1999**, *283*, 1148–1150.
- (6) Li, H.; Eddaoudi, M.; O’Keeffe, M.; Yaghi, O. M. Design and synthesis of an exceptionally stable and highly porous metal-organic framework. *Nature* **1999**, *402*, 276–279.
- (7) Moghadam, P. Z.; Li, A.; Wiggin, S. B.; Tao, A.; Maloney, A. G. P.; Wood, P. A.; Ward, S. C.; Fairen-Jimenez, D. Development of a Cambridge Structural Database Subset: A Collection of Metal–Organic Frameworks for Past, Present, and Future. *Chem. Mater.* **2017**, *29*, 2618–2625.
- (8) Cavka, J. H.; Jakobsen, S.; Olsbye, U.; Guillou, N.; Lamberti, C.; Bordiga, S.; Lillerud, K. P. A New Zirconium Inorganic Building Brick Forming Metal Organic Frameworks with Exceptional Stability. *J. Am. Chem. Soc.* **2008**, *130*, 13850–13851.
- (9) Serra-Crespo, P.; Ramos-Fernandez, E. V.; Gascon, J.; Kapteijn, F. Synthesis and Characterization of an Amino Functionalized MIL-

101(Al): Separation and Catalytic Properties. *Chem. Mater.* **2011**, *23*, 2565–2572.

(10) Dan-Hardi, M.; Serre, C.; Frot, T.; Rozes, L.; Maurin, G.; Sanchez, C.; Férey, G. A New Photoactive Crystalline Highly Porous Titanium(IV) Dicarboxylate. *J. Am. Chem. Soc.* **2009**, *131*, 10857–10859.

(11) Wu, Y.-P.; Tian, J.-W.; Liu, S.; Li, B.; Zhao, J.; Ma, L.-F.; Li, D.-S.; Lan, Y.-Q.; Bu, X. Bi-Microporous Metal–Organic Frameworks with Cubane $[M_4(OH)_4]$ ($M = Ni, Co$) Clusters and Pore-Space Partition for Electrocatalytic Methanol Oxidation Reaction. *Angew. Chem., Int. Ed.* **2019**, *58*, 12185–12189.

(12) Suga, M.; Akita, F.; Yamashita, K.; Nakajima, Y.; Ueno, G.; Li, H.; Yamane, T.; Hirata, K.; Umena, Y.; Yonekura, S.; Yu, L.-J.; Murakami, H.; Nomura, T.; Kimura, T.; Kubo, M.; Baba, S.; Kumasaka, T.; Tono, K.; Yabashi, M.; Isobe, H.; Yamaguchi, K.; Yamamoto, M.; Ago, H.; Shen, J.-R. An oxyl/oxo mechanism for oxygen-oxygen coupling in PSII revealed by an X-ray free-electron laser. *Science* **2019**, *366*, 334–338.

(13) Bennett, T. D.; Cheetham, A. K.; Fuchs, A. H.; Coudert, F.-X. Interplay between defects, disorder and flexibility in metal-organic frameworks. *Nat. Chem.* **2017**, *9*, 11–16.

(14) Dissegna, S.; Epp, K.; Heinz, W. R.; Kieslich, G.; Fischer, R. A. Defective Metal–Organic Frameworks. *Adv. Mater.* **2018**, *30*, 1704501–1704524.

(15) Klet, R. C.; Liu, Y.; Wang, T. C.; Hupp, J. T.; Farha, O. K. Evaluation of Brønsted acidity and proton topology in Zr- and Hf-based metal–organic frameworks using potentiometric acid–base titration. *J. Mater. Chem. A* **2016**, *4*, 1479–1485.

(16) Planas, N.; Mondloch, J. E.; Tussupbayev, S.; Borycz, J.; Gagliardi, L.; Hupp, J. T.; Farha, O. K.; Cramer, C. J. Defining the Proton Topology of the Zr_6 -Based Metal–Organic Framework NU-1000. *J. Phys. Chem. Lett.* **2014**, *5*, 3716–3723.

(17) Furukawa, H.; Müller, U.; Yaghi, O. M. “Heterogeneity within Order” in Metal–Organic Frameworks. *Angew. Chem., Int. Ed.* **2015**, *54*, 3417–3430.

(18) Vermoortele, F.; Bueken, B.; Le Bars, G.; Van de Voorde, B.; Vandichel, M.; Houthoofd, K.; Vimont, A.; Daturi, M.; Waroquier, M.; Van Speybroeck, V.; Kirschhock, C.; De Vos, D. E. Synthesis Modulation as a Tool to Increase the Catalytic Activity of Metal–Organic Frameworks: The Unique Case of UiO-66(Zr). *J. Am. Chem. Soc.* **2013**, *135*, 11465–11468.

(19) Shearer, G. C.; Chavan, S.; Bordiga, S.; Svelle, S.; Olsbye, U.; Lillerud, K. P. Defect Engineering: Tuning the Porosity and Composition of the Metal–Organic Framework UiO-66 via Modulated Synthesis. *Chem. Mater.* **2016**, *28*, 3749–3761.

(20) Schaate, A.; Roy, P.; Godt, A.; Lippke, J.; Waltz, F.; Wiebcke, M.; Behrens, P. Modulated Synthesis of Zr-Based Metal–Organic Frameworks: From Nano to Single Crystals. *Chem. - Eur. J.* **2011**, *17*, 6643–6651.

(21) Katz, M. J.; Brown, Z. J.; Colón, Y. J.; Siu, P. W.; Scheidt, K. A.; Snurr, R. Q.; Hupp, J. T.; Farha, O. K. A facile synthesis of UiO-66, UiO-67 and their derivatives. *Chem. Commun.* **2013**, *49*, 9449–9451.

(22) Yang, D.; Ortuño, M. A.; Bernales, V.; Cramer, C. J.; Gagliardi, L.; Gates, B. C. Structure and Dynamics of Zr_6O_8 Metal–Organic Framework Node Surfaces Probed with Ethanol Dehydration as a Catalytic Test Reaction. *J. Am. Chem. Soc.* **2018**, *140*, 3751–3759.

(23) DeCoste, J. B.; Demasky, T. J.; Katz, M. J.; Farha, O. K.; Hupp, J. T. A UiO-66 analogue with uncoordinated carboxylic acids for the broad-spectrum removal of toxic chemicals. *New J. Chem.* **2015**, *39*, 2396–2399.

(24) Islamoglu, T.; Goswami, S.; Li, Z.; Howarth, A. J.; Farha, O. K.; Hupp, J. T. Postsynthetic Tuning of Metal–Organic Frameworks for Targeted Applications. *Acc. Chem. Res.* **2017**, *50*, 805–813.

(25) Yang, D.; Gaggioli, C. A.; Ray, D.; Babucci, M.; Gagliardi, L.; Gates, B. C. Tuning Catalytic Sites on Zr_6O_8 Metal–Organic Framework Nodes via Ligand and Defect Chemistry Probed with *tert*-Butyl Alcohol Dehydration to Isobutylene. *J. Am. Chem. Soc.* **2020**, *142*, 8044–8056.

(26) Yang, D.; Bernales, V.; Islamoglu, T.; Farha, O. K.; Hupp, J. T.; Cramer, C. J.; Gagliardi, L.; Gates, B. C. Tuning the Surface Chemistry of Metal Organic Framework Nodes: Proton Topology of the Metal-Oxide-Like Zr_6 Nodes of UiO-66 and NU-1000. *J. Am. Chem. Soc.* **2016**, *138*, 15189–15196.

(27) Ravon, U.; Domine, M. E.; Gaudillere, C.; Desmartin-Chomel, A.; Farrusseng, D. MOFs as acid catalysts with shape selectivity properties. *New J. Chem.* **2008**, *32*, 937–940.

(28) Ravon, U.; Savonnet, M.; Aguado, S.; Domine, M. E.; Janneau, E.; Farrusseng, D. Engineering of coordination polymers for shape selective alkylation of large aromatics and the role of defects. *Micropor. Mesopor. Mater.* **2010**, *129*, 319–329.

(29) Canivet, J.; Vandichel, M.; Farrusseng, D. Origin of highly active metal–organic framework catalysts: Defects? Defects! *Dalton Trans.* **2016**, *45*, 4090–4099.

(30) Bai, Y.; Dou, Y. B.; Xie, L. H.; Rutledge, W.; Li, J. R.; Zhou, H. C. Zr-based metal–organic frameworks: design, synthesis, structure, and applications. *Chem. Soc. Rev.* **2016**, *45*, 2327–2367.

(31) Wu, H.; Chua, Y. S.; Krungleviciute, V.; Tyagi, M.; Chen, P.; Yildirim, T.; Zhou, W. Unusual and Highly Tunable Missing-Linker Defects in Zirconium Metal–Organic Framework UiO-66 and Their Important Effects on Gas Adsorption. *J. Am. Chem. Soc.* **2013**, *135*, 10525–10532.

(32) Cliffe, M. J.; Wan, W.; Zou, X.; Chater, P. A.; Kleppe, A. K.; Tucker, M. G.; Wilhelm, H.; Funnell, N. P.; Coudert, F.-X.; Goodwin, A. L. Correlated defect nanoregions in a metal–organic framework. *Nat. Commun.* **2014**, *5*, 4176.

(33) Gutterød, E. S.; Lazzarini, A.; Fjermestad, T.; Kaur, G.; Manzoli, M.; Bordiga, S.; Svelle, S.; Lillerud, K. P.; Skúlason, E.; Øien-Ødegaard, S.; Nova, A.; Olsbye, U. Hydrogenation of CO_2 to Methanol by Pt Nanoparticles Encapsulated in UiO-67: Deciphering the Role of the Metal–Organic Framework. *J. Am. Chem. Soc.* **2020**, *142*, 999–1009.

(34) Vimont, A.; Leclerc, H.; Maugé, F.; Daturi, M.; Lavalley, J.-C.; Surblé, S.; Serre, C.; Férey, G. Creation of Controlled Brønsted Acidity on a Zeotypic Mesoporous Chromium(III) Carboxylate by Grafting Water and Alcohol Molecules. *J. Phys. Chem. C* **2007**, *111*, 383–388.

(35) Bernales, V.; Ortuño, M. A.; Truhlar, D. G.; Cramer, C. J.; Gagliardi, L. Computational Design of Functionalized Metal–Organic Framework Nodes for Catalysis. *ACS Cent. Sci.* **2018**, *4*, 5–19.

(36) Katz, M. J.; Moon, S.-Y.; Mondloch, J. E.; Beyzavi, M. H.; Stephenson, C. J.; Hupp, J. T.; Farha, O. K. Exploiting parameter space in MOFs: a 20-fold enhancement of phosphate-ester hydrolysis with UiO-66- NH_2 . *Chem. Sci.* **2015**, *6*, 2286–2291.

(37) Caratelli, C.; Hajek, J.; Cirujano, F. G.; Waroquier, M.; Llabrés i Xamena, F. X.; Van Speybroeck, V. Nature of active sites on UiO-66 and beneficial influence of water in the catalysis of Fischer esterification. *J. Catal.* **2017**, *352*, 401–414.

(38) Blandez, J. F.; Santiago-Portillo, A.; Navalon, S.; Gimenez-Marques, M.; Alvaro, M.; Horcajada, P.; Garcia, H. Influence of functionalization of terephthalate linker on the catalytic activity of UiO-66 for epoxide ring opening. *J. Mol. Catal. A: Chem.* **2016**, *425*, 332–339.

(39) Chen, X.; Lyu, Y.; Wang, Z.; Qiao, X.; Gates, B. C.; Yang, D. Tuning $Zr_{12}O_{22}$ Node Defects as Catalytic Sites in the Metal–Organic Framework hcp UiO-66. *ACS Catal.* **2020**, *10*, 2906–2914.

(40) Lustemberg, P. G.; Bosco, M. V.; Bonivardi, A.; Busnengo, H. F.; Ganduglia-Pirovano, M. V. Insights into the Nature of Formate Species in the Decomposition and Reaction of Methanol over Cerium Oxide Surfaces: A Combined Infrared Spectroscopy and Density Functional Theory Study. *J. Phys. Chem. C* **2015**, *119*, 21452–21464.

(41) Rotzinger, F. P.; Kesselman-Truttmann, J. M.; Hug, S. J.; Shklover, V.; Grätzel, M. Structure and Vibrational Spectrum of Formate and Acetate Adsorbed from Aqueous Solution onto the TiO_2 Rutile (110) Surface. *J. Phys. Chem. B* **2004**, *108*, 5004–5017.

(42) Hadjivanov, K. Identification and Characterization of Surface Hydroxyl Groups by Infrared Spectroscopy. In *Adv. Catal.*; Jentoft, F. C., Ed.; Academic Press, 2014; Vol. 57, Chapter 2, pp 99–318.

- (43) Jung, K. T.; Bell, A. T. An in Situ Infrared Study of Dimethyl Carbonate Synthesis from Carbon Dioxide and Methanol over Zirconia. *J. Catal.* **2001**, *204*, 339–347.
- (44) Trickett, C. A.; Osborn Popp, T. M.; Su, J.; Yan, C.; Weisberg, J.; Huq, A.; Urban, P.; Jiang, J.; Kalmutzi, M. J.; Liu, Q.; Baek, J.; Head-Gordon, M. P.; Somorjai, G. A.; Reimer, J. A.; Yaghi, O. M. Identification of the strong Brønsted acid site in a metal–organic framework solid acid catalyst. *Nat. Chem.* **2019**, *11*, 170–176.
- (45) Zuo, Q.; Liu, T.; Chen, C.; Ji, Y.; Gong, X.; Mai, Y.; Zhou, Y. Ultrathin Metal–Organic Framework Nanosheets with Ultrahigh Loading of Single Pt Atoms for Efficient Visible-Light-Driven Photocatalytic H₂ Evolution. *Angew. Chem., Int. Ed.* **2019**, *58*, 10198–10203.
- (46) Fang, X.; Shang, Q.; Wang, Y.; Jiao, L.; Yao, T.; Li, Y.; Zhang, Q.; Luo, Y.; Jiang, H.-L. Single Pt Atoms Confined into a Metal–Organic Framework for Efficient Photocatalysis. *Adv. Mater.* **2018**, *30*, 1705112–1705119.
- (47) Yang, D.; Odoh, S. O.; Wang, T. C.; Farha, O. K.; Hupp, J. T.; Cramer, C. J.; Gagliardi, L.; Gates, B. C. Metal–Organic Framework Nodes as Nearly Ideal Supports for Molecular Catalysts: NU-1000 and UiO-66-Supported Iridium Complexes. *J. Am. Chem. Soc.* **2015**, *137*, 7391–7396.
- (48) Yang, D.; Odoh, S. O.; Borycz, J.; Wang, T. C.; Farha, O. K.; Hupp, J. T.; Cramer, C. J.; Gagliardi, L.; Gates, B. C. Tuning Zr₆ Metal–Organic Framework (MOF) Nodes as Catalyst Supports: Site Densities and Electron-Donor Properties Influence Molecular Iridium Complexes as Ethylene Conversion Catalysts. *ACS Catal.* **2016**, *6*, 235–247.
- (49) Bernales, V.; Yang, D.; Yu, J.; Gümüşlü, G.; Cramer, C. J.; Gates, B. C.; Gagliardi, L. Molecular Rhodium Complexes Supported on the Metal-Oxide-Like Nodes of Metal Organic Frameworks and on Zeolite HY: Catalysts for Ethylene Hydrogenation and Dimerization. *ACS Appl. Mater. Interfaces* **2017**, *9*, 33511–33520.
- (50) Geng, K.; He, T.; Liu, R.; Dalapati, S.; Tan, K. T.; Li, Z.; Tao, S.; Gong, Y.; Jiang, Q.; Jiang, D., Covalent Organic Frameworks: Design, Synthesis, and Functions. *Chem. Rev.* **2020**, in press. DOI: 10.1021/acs.chemrev.9b00550.
- (51) Islamoglu, T.; Ortuño, M. A.; Prussaloglou, E.; Howarth, A. J.; Vermeulen, N. A.; Atilgan, A.; Asiri, A. M.; Cramer, C. J.; Farha, O. K. Presence versus Proximity: The Role of Pendant Amines in the Catalytic Hydrolysis of a Nerve Agent Simulant. *Angew. Chem., Int. Ed.* **2018**, *57*, 1949–1953.
- (52) Groups on MOF linkers even influence catalysis on metal nanoparticles encapsulated in MOF pores, possibly by interacting directly with the clusters. For example, COOH groups on BDC linkers of UiO-66 markedly increased the catalytic activity of copper clusters in UiO-66 for CO₂ hydrogenation to methanol, and (CH₃)₂ groups on BDC linkers of UiO-66 increased the activity of platinum clusters for the water–gas shift reaction. Much remains to be understood about these effects. Kobayashi, H.; Taylor, J. M.; Mitsuka, Y.; Ogiwara, N.; Yamamoto, T.; Toriyama, T.; Matsumura, S.; Kitagawa, H. *Chem. Sci.* **2019**, *10*, 3289–3294. Ogiwara, N.; Kobayashi, H.; Inukai, M.; Nishiyama, Y.; Concepción, P.; Rey, F.; Kitagawa, H. *Nano Lett.* **2020**, *20*, 426–432.
- (53) Kim, J.; Rees, D. C. Structural Models for the Metal Centers in the Nitrogenase Molybdenum-Iron Protein. *Science* **1992**, *257*, 1677–1682.
- (54) Zhang, B.; Sun, L. Why nature chose the Mn₄CaO₅ cluster as water-splitting catalyst in photosystem II: a new hypothesis for the mechanism of O–O bond formation. *Dalton Trans.* **2018**, *47*, 14381–14387.
- (55) Zhai, Q.-G.; Bu, X.; Mao, C.; Zhao, X.; Feng, P. Systematic and Dramatic Tuning on Gas Sorption Performance in Heterometallic Metal–Organic Frameworks. *J. Am. Chem. Soc.* **2016**, *138*, 2524–2527.
- (56) Zhai, Q.-G.; Bu, X.; Mao, C.; Zhao, X.; Daemen, L.; Cheng, Y.; Ramirez-Cuesta, A. J.; Feng, P. An ultra-tunable platform for molecular engineering of high-performance crystalline porous materials. *Nat. Commun.* **2016**, *7*, 13645–13653.
- (57) Yang, H.; Wang, Y.; Krishna, R.; Jia, X.; Wang, Y.; Hong, A. N.; Dang, C.; Castillo, H. E.; Bu, X.; Feng, P. Pore-Space-Partition-Enabled Exceptional Ethane Uptake and Ethane-Selective Ethane–Ethylene Separation. *J. Am. Chem. Soc.* **2020**, *142*, 2222–2227.
- (58) Masoomi, M. Y.; Morsali, A.; Dhakshinamoorthy, A.; Garcia, H. Mixed-Metal MOFs: Unique Opportunities in Metal–Organic Framework (MOF) Functionality and Design. *Angew. Chem., Int. Ed.* **2019**, *58*, 15188–15205.
- (59) Abednatanzi, S.; Gohari Derakhshandeh, P.; Depauw, H.; Coudert, F.-X.; Vrielinck, H.; Van Der Voort, P.; Leus, K. Mixed-metal metal–organic frameworks. *Chem. Soc. Rev.* **2019**, *48*, 2535–2565.
- (60) Osadchii, D. Y.; Olivos-Suarez, A. I.; Szécsényi, Á.; Li, G.; Nasalevich, M. A.; Dugulan, I. A.; Crespo, P. S.; Hensen, E. J. M.; Veber, S. L.; Fedin, M. V.; Sankar, G.; Pidko, E. A.; Gascon, J. Isolated Fe Sites in Metal Organic Frameworks Catalyze the Direct Conversion of Methane to Methanol. *ACS Catal.* **2018**, *8*, 5542–5548.
- (61) Santaclara, J. G.; Olivos-Suarez, A. I.; Gonzalez-Nelson, A.; Osadchii, D.; Nasalevich, M. A.; van der Veen, M. A.; Kapteijn, F.; Sheveleva, A. M.; Veber, S. L.; Fedin, M. V.; Murray, A. T.; Hendon, C. H.; Walsh, A.; Gascon, J. Revisiting the Incorporation of Ti(IV) in UiO-type Metal–Organic Frameworks: Metal Exchange versus Grafting and Their Implications on Photocatalysis. *Chem. Mater.* **2017**, *29*, 8963–8967.
- (62) Korzyński, M. D.; Braglia, L.; Borfecchia, E.; Lomachenko, K. A.; Baldansuren, A.; Hendon, C. H.; Lamberti, C.; Dincă, M. Quo vadis niobium? Divergent coordination behavior of early-transition metals towards MOF-5. *Chem. Sci.* **2019**, *10*, 5906–5910.
- (63) MOF nodes have also been modified by postsynthetic treatments. For example, [Zn₄O]⁶⁺ is prone to exchanging Zn²⁺ for most first-row transition metal ions in various oxidation states. MOF-5 was therefore identified as a promising candidate for exploring niobium chemistry, but instead of such exchange, niobium was found to decorate nodes with Nb(V).⁶² There are numerous examples of grafting of metal complexes to MOF nodes. (See ref 24.)
- (64) Song, F.; Al-Ameed, K.; Schilling, M.; Fox, T.; Luber, S.; Patzke, G. R. Mechanistically Driven Control over Cubane Oxo Cluster Catalysts. *J. Am. Chem. Soc.* **2019**, *141*, 8846–8857.
- (65) Li, J.; Wan, W.; Triana, C. A.; Novotny, Z.; Osterwalder, J.; Erni, R.; Patzke, G. R. Dynamic Role of Cluster Cocatalysts on Molecular Photoanodes for Water Oxidation. *J. Am. Chem. Soc.* **2019**, *141*, 12839–12848.
- (66) Nguyen, A. I.; Darago, L. E.; Balcells, D.; Tilley, T. D. Influence of a “Dangling” Co(II) Ion Bound to a [MnCo₃O₄] Oxo Cubane. *J. Am. Chem. Soc.* **2018**, *140*, 9030–9033.
- (67) Olshansky, L.; Huerta-Lavorie, R.; Nguyen, A. I.; Vallapurackal, J.; Furst, A.; Tilley, T. D.; Borovik, A. S. Artificial Metalloproteins Containing Co₄O₄ Cubane Active Sites. *J. Am. Chem. Soc.* **2018**, *140*, 2739–2742.
- (68) Nguyen, A. I.; Van Allsburg, K. M.; Terban, M. W.; Bajdich, M.; Oktawiec, J.; Amtawong, J.; Ziegler, M. S.; Dombrowski, J. P.; Lakshmi, K. V.; Drisdell, W. S.; Yano, J.; Billinge, S. J. L.; Tilley, T. D. Stabilization of reactive Co₄O₄ cubane oxygen-evolution catalysts within porous frameworks. *Proc. Natl. Acad. Sci. U. S. A.* **2019**, *116*, 11630–11639.
- (69) Brodsky, C. N.; Hadt, R. G.; Hayes, D.; Reinhart, B. J.; Li, N.; Chen, L. X.; Nocera, D. G. In situ characterization of cofacial Co(IV) centers in Co₄O₄ cubane: Modeling the high-valent active site in oxygen-evolving catalysts. *Proc. Natl. Acad. Sci. U. S. A.* **2017**, *114*, 3855–3860.
- (70) Gerken, J. B.; McAlpin, J. G.; Chen, J. Y. C.; Rigsby, M. L.; Casey, W. H.; Britt, R. D.; Stahl, S. S. Electrochemical Water Oxidation with Cobalt-Based Electrocatalysts from pH 0–14: The Thermodynamic Basis for Catalyst Structure, Stability, and Activity. *J. Am. Chem. Soc.* **2011**, *133*, 14431–14442.
- (71) McAlpin, J. G.; Surendranath, Y.; Dincă, M.; Stich, T. A.; Stoian, S. A.; Casey, W. H.; Nocera, D. G.; Britt, R. D. EPR Evidence

for Co(IV) Species Produced During Water Oxidation at Neutral pH. *J. Am. Chem. Soc.* **2010**, *132*, 6882–6883.

(72) Hocking, R. K.; Brimblecombe, R.; Chang, L. Y.; Singh, A.; Cheah, M. H.; Glover, C.; Casey, W. H.; Spiccia, L. Water-oxidation catalysis by manganese in a geochemical-like cycle. *Nat. Chem.* **2011**, *3*, 461–466.

(73) Loiseau, T.; Serre, C.; Huguenard, C.; Fink, G.; Taulelle, F.; Henry, M.; Bataille, T.; Férey, G. A Rationale for the Large Breathing of the Porous Aluminum Terephthalate (MIL-53) upon Hydration. *Chem. - Eur. J.* **2004**, *10*, 1373–1382.

(74) Burtch, N. C.; Jasuja, H.; Walton, K. S. Water Stability and Adsorption in Metal–Organic Frameworks. *Chem. Rev.* **2014**, *114*, 10575–10612.

(75) Geletii, Y. V.; Besson, C.; Hou, Y.; Yin, Q.; Musaev, D. G.; Quiñero, D.; Cao, R.; Hardcastle, K. I.; Proust, A.; Kögerler, P.; Hill, C. L. Structural, Physicochemical, and Reactivity Properties of an All-Inorganic, Highly Active Tetra-ruthenium Homogeneous Catalyst for Water Oxidation. *J. Am. Chem. Soc.* **2009**, *131*, 17360–17370.

(76) Bonchio, M.; Syrgiannis, Z.; Burian, M.; Marino, N.; Pizzolato, E.; Dirian, K.; Rigodanza, F.; Volpato, G. A.; La Ganga, G.; Demitri, N.; Berardi, S.; Amenitsch, H.; Guldi, D. M.; Caramori, S.; Bignozzi, C. A.; Sartorel, A.; Prato, M. Hierarchical organization of perylene bisimides and polyoxometalates for photo-assisted water oxidation. *Nat. Chem.* **2019**, *11*, 146–153.

(77) Åberg, M.; Glaser, J. ¹⁷O and ¹H NMR study of the tetranuclear hydroxo zirconium complex in aqueous solution. *Inorg. Chim. Acta* **1993**, *206*, 53–61.

(78) Wang, S.-S.; Yang, G.-Y. Recent Advances in Polyoxometalate-Catalyzed Reactions. *Chem. Rev.* **2015**, *115*, 4893–4962.

(79) Lv, H.; Song, J.; Geletii, Y. V.; Vickers, J. W.; Sumliner, J. M.; Musaev, D. G.; Kögerler, P.; Zhuk, P. F.; Bacsa, J.; Zhu, G.; Hill, C. L. An Exceptionally Fast Homogeneous Carbon-Free Cobalt-Based Water Oxidation Catalyst. *J. Am. Chem. Soc.* **2014**, *136*, 9268–9271.

(80) Delgado, O.; Dress, A.; Müller, A.; Pope, M. T. Polyoxometalates: A Class of Compounds with Remarkable Topology. In *Polyoxometalates: From Platonic Solids to Anti-Retroviral Activity*; Pope, M. T., Müller, A., Eds.; Springer Netherlands: Dordrecht, 1994; pp 7–26.

(81) Weinstock, I. A.; Schreiber, R. E.; Neumann, R. Dioxxygen in Polyoxometalate Mediated Reactions. *Chem. Rev.* **2018**, *118*, 2680–2717.

(82) Casey, W. H. Oxygen–Isotope Exchange and Metastable Dissociation in Oxides. In *Adv. Inorg. Chem.*; van Eldik, R., Cronin, L., Eds.; Academic Press, 2017; Vol. 69, Chapter 4, pp 91–115.

(83) Miras, H. N.; Vilà-Nadal, L.; Cronin, L. Polyoxometalate based open-frameworks (POM-OFs). *Chem. Soc. Rev.* **2014**, *43*, 5679–5699.

(84) López, X.; Carbó, J. J.; Bo, C.; Poblet, J. M. Structure, properties and reactivity of polyoxometalates: a theoretical perspective. *Chem. Soc. Rev.* **2012**, *41*, 7537–7571.

(85) Misra, A.; Kozma, K.; Streb, C.; Nyman, M. Beyond Charge Balance: Counter-Cations in Polyoxometalate Chemistry. *Angew. Chem., Int. Ed.* **2020**, *59*, 596–612.

(86) Rowsell, J.; Nazar, L. F. Speciation and Thermal Transformation in Alumina Sols: Structures of the Polyhydroxyoxoaluminum Cluster $[Al_{30}O_8(OH)_{56}(H_2O)_{26}]^{18+}$ and Its δ -Keggin Moiety. *J. Am. Chem. Soc.* **2000**, *122*, 3777–3778.

(87) Sadeghi, O.; Zakharov, L. N.; Nyman, M. Aqueous formation and manipulation of the iron-oxo Keggin ion. *Science* **2015**, *347*, 1359–1362.

(88) Smart, S. E.; Vaughn, J.; Pappas, I.; Pan, L. Controlled step-wise isomerization of the Keggin-type Al_{13} and determination of the γ - Al_{13} structure. *Chem. Commun.* **2013**, *49*, 11352–11354.

(89) Deschaume, O.; Breynaert, E.; Radhakrishnan, S.; Kerkhofs, S.; Haouas, M.; Adam de Beaumais, S.; Manzin, V.; Galey, J. B.; Ramos-Stanbury, L.; Taulelle, F.; Martens, J. A.; Batic, C. Impact of Amino Acids on the Isomerization of the Aluminum Tridecamer $Al(13)$. *Inorg. Chem.* **2017**, *56*, 12401–12409.

(90) Helm, L.; Merbach, A. E. Inorganic and Bioinorganic Solvent Exchange Mechanisms. *Chem. Rev.* **2005**, *105*, 1923–1960.

(91) Wang, J.; Rustad, J. R.; Casey, W. H. Calculation of Water-Exchange Rates on Aqueous Polynuclear Clusters and at Oxide–Water Interfaces. *Inorg. Chem.* **2007**, *46*, 2962–2964.

(92) Yu, P.; Lee, A. P.; Phillips, B. L.; Casey, W. H. Potentiometric and ¹⁹F nuclear magnetic resonance spectroscopic study of fluoride substitution in the $GaAl_{12}$ polyoxocation: implications for aluminum (hydr)oxide mineral surfaces. *Geochim. Cosmochim. Acta* **2003**, *67*, 1065–1080.

(93) Casey, W. H. Large Aqueous Aluminum Hydroxide Molecules. *Chem. Rev.* **2006**, *106*, 1–16.

(94) Villa, E. M.; Ohlin, C. A.; Casey, W. H. Oxygen-Isotope Exchange Rates for Three Isostructural Polyoxometalate Ions. *J. Am. Chem. Soc.* **2010**, *132*, 5264–5272.

(95) Rustad, J. R. Elementary Reactions in Polynuclear Ions and Aqueous–Mineral Interfaces: A New Geology. In *Adv. Inorg. Chem.*; van Eldik, R., Harvey, J., Eds.; Academic Press, 2010; Vol. 62, pp 391–436.

(96) Minato, T.; Suzuki, K.; Yamaguchi, K.; Mizuno, N. Alkoxides of Trivacant Lacunary Polyoxometalates. *Chem. - Eur. J.* **2017**, *23*, 14213–14220.

(97) Long, D.-L.; Burkholder, E.; Cronin, L. Polyoxometalate clusters, nanostructures and materials: From self assembly to designer materials and devices. *Chem. Soc. Rev.* **2007**, *36*, 105–121.

(98) Boyd, T.; Mitchell, S. G.; Gabb, D.; Long, D.-L.; Song, Y.-F.; Cronin, L. POMzites: A Family of Zeolitic Polyoxometalate Frameworks from a Minimal Building Block Library. *J. Am. Chem. Soc.* **2017**, *139*, 5930–5938.

(99) Deshlahra, P.; Iglesia, E. Toward More Complete Descriptors of Reactivity in Catalysis by Solid Acids. *ACS Catal.* **2016**, *6*, 5386–5392.

(100) Macht, J.; Iglesia, E. Structure and function of oxide nanostructures: catalytic consequences of size and composition. *Phys. Chem. Chem. Phys.* **2008**, *10*, 5331–5343.

(101) Macht, J.; Janik, M. J.; Neurock, M.; Iglesia, E. Mechanistic Consequences of Composition in Acid Catalysis by Polyoxometalate Keggin Clusters. *J. Am. Chem. Soc.* **2008**, *130*, 10369–10379.

(102) Gumerova, N. I.; Rompel, A. Synthesis, structures and applications of electron-rich polyoxometalates. *Nat. Rev. Chem.* **2018**, *2*, 0112–0124.

(103) Haviv, E.; Shimon, L. J. W.; Neumann, R. Photochemical Reduction of CO₂ with Visible Light Using a Polyoxometalate as Photoreductant. *Chem. - Eur. J.* **2017**, *23*, 92–95.

(104) Miras, H. N.; Yan, J.; Long, D.-L.; Cronin, L. Engineering polyoxometalates with emergent properties. *Chem. Soc. Rev.* **2012**, *41*, 7403–7430.

(105) Kondinski, A.; Parac-Vogt, T. N. Keggin Structure, Qu \bar{o} V \bar{a} dis? *Front. Chem.* **2018**, *6*, 1–7.

(106) Du, D.-Y.; Qin, J.-S.; Li, S.-L.; Su, Z.-M.; Lan, Y.-Q. Recent advances in porous polyoxometalate-based metal–organic framework materials. *Chem. Soc. Rev.* **2014**, *43*, 4615–4632.

(107) Li, X.-X.; Zhao, D.; Zheng, S.-T. Recent advances in POM-organic frameworks and POM-organic polyhedra. *Coord. Chem. Rev.* **2019**, *397*, 220–240.

(108) Dolbecq, A.; Mellot-Draznieks, C.; Mialane, P.; Marrot, J.; Férey, G.; Sécheresse, F. Hybrid 2D and 3D Frameworks Based on ϵ -Keggin Polyoxometalates: Experiment and Simulation. *Eur. J. Inorg. Chem.* **2005**, *2005*, 3009–3018.

(109) Marleny Rodriguez-Albelo, L.; Ruiz-Salvador, A. R.; Sampieri, A.; Lewis, D. W.; Gómez, A.; Nohra, B.; Mialane, P.; Marrot, J.; Sécheresse, F.; Mellot-Draznieks, C.; Ngo Biboum, R.; Keita, B.; Nadjo, L.; Dolbecq, A. Zeolitic Polyoxometalate-Based Metal–Organic Frameworks (Z-POMOFs): Computational Evaluation of Hypothetical Polymorphs and the Successful Targeted Synthesis of the Redox-Active Z-POMOF1. *J. Am. Chem. Soc.* **2009**, *131*, 16078–16087.

(110) Vilà-Nadal, L.; Cronin, L. Design and synthesis of polyoxometalate-framework materials from cluster precursors. *Nat. Rev. Mater.* **2017**, *2*, 17054–17069.

(111) Zheng, S.-T.; Zhang, J.; Li, X.-X.; Fang, W.-H.; Yang, G.-Y. Cubic Polyoxometalate–Organic Molecular Cage. *J. Am. Chem. Soc.* **2010**, *132*, 15102–15103.

(112) Shearer, G. C.; Chavan, S.; Ethiraj, J.; Vitillo, J. G.; Svelle, S.; Olsbye, U.; Lamberti, C.; Bordiga, S.; Lillerud, K. P. Tuned to Perfection: Ironing Out the Defects in Metal–Organic Framework UiO-66. *Chem. Mater.* **2014**, *26*, 4068–4071.

(113) Beyzavi, M. H.; Klet, R. C.; Tussupbayev, S.; Borycz, J.; Vermeulen, N. A.; Cramer, C. J.; Stoddart, J. F.; Hupp, J. T.; Farha, O. K. A Hafnium-Based Metal–Organic Framework as an Efficient and Multifunctional Catalyst for Facile CO₂ Fixation and Regioselective and Enantioselective Epoxide Activation. *J. Am. Chem. Soc.* **2014**, *136*, 15861–15864.

(114) Rieth, A. J.; Wright, A. M.; Dincă, M. Kinetic stability of metal–organic frameworks for corrosive and coordinating gas capture. *Nat. Rev. Mater.* **2019**, *4*, 708–725.

(115) Wang, Y.; Wöll, C. Chemical Reactions at Isolated Single-Sites Inside Metal–Organic Frameworks. *Catal. Lett.* **2018**, *148*, 2201–2222.

(116) Müller, A.; Gouzerh, P. From linking of metal-oxide building blocks in a dynamic library to giant clusters with unique properties and towards adaptive chemistry. *Chem. Soc. Rev.* **2012**, *41*, 7431–7463.

(117) Cowan, J. J.; Bailey, A. J.; Heintz, R. A.; Do, B. T.; Hardcastle, K. I.; Hill, C. L.; Weinstock, I. A. Formation, isomerization, and derivatization of Keggin tungstoaluminates. *Inorg. Chem.* **2001**, *40*, 6666–6675.

(118) Weinstock, I. A.; Cowan, J. J.; Barbuzzi, E. M. G.; Zeng, H.; Hill, C. L. Equilibria between α and β Isomers of Keggin Heteropolytungstates. *J. Am. Chem. Soc.* **1999**, *121*, 4608–4617.

(119) Yuan, S.; Feng, L.; Wang, K. C.; Pang, J. D.; Bosch, M.; Lollar, C.; Sun, Y. J.; Qin, J. S.; Yang, X. Y.; Zhang, P.; Wang, Q.; Zou, L. F.; Zhang, Y. M.; Zhang, L. L.; Fang, Y.; Li, J. L.; Zhou, H. C. Stable Metal–Organic Frameworks: Design, Synthesis, and Applications. *Adv. Mater.* **2018**, *30*, 1704303–1704310.